**Atmospheric
Chemistry
and Physics
Discussions**

Comparison and
synergy of
stratospheric ozone
measurements

K. Hocke et al.

Comparison and synergy of stratospheric ozone measurements by satellite limb sounders and the ground-based microwave radiometer SOMORA

K. Hocke[1], N. Kämpfer[1], D. Ruffieux[2], L. Froidevaux[3], A. Parrish[4], I. Boyd[4], T. von Clarmann[5], T. Steck[5], Y.M. Timofeyev[6], A.V. Polyakov[6], and E. Kyrölä[7]

[1]Institute of Applied Physics, University of Bern, Switzerland
[2]MeteoSwiss, Payerne, Switzerland
[3]Jet Propulsion Laboratory, California Institute of Technology, Pasadena, USA
[4]University of Massachusetts, USA
[5]Institut für Meteorologie und Klimaforschung, Forschungszentrum Karlsruhe und Universität Karlsruhe, Germany
[6]Department of Atmospheric Physics, St. Petersburg State University, Russia
[7]Finnish Meteorological Institute, Helsinki, Finland

Correspondence to: K. Hocke (klemens.hocke@mw.iap.unibe.ch)

Title Page

Abstract	Introduction
Conclusions	References
Tables	Figures

| I◄ | ►I |
| ◄ | ► |

| Back | Close |

Full Screen / Esc

Printer-friendly Version

Interactive Discussion

EGU

Abstract

Stratospheric O_3 profiles obtained by the satellite limb sounders Aura/MLS, ENVISAT/MIPAS, ENVISAT/GOMOS, SAGE-II, SAGE-III, UARS/HALOE are compared to coincident O_3 profiles of the ground-based microwave radiometer SOMORA in Switzerland. Data from the various measurement techniques are within 10% at altitudes below 45 km. At altitudes 45–60 km, the relative O_3 differences are within a range of 50%. Larger deviations at upper altitudes are attributed to larger relative measurement errors caused by lower O_3 concentrations. The spatiotemporal characteristics of the O_3 differences (satellite – ground station) are investigated by analyzing about 5000 coincident profile pairs of Aura/MLS (retrieval version 1.5) and SOMORA. The probability density function of the O_3 differences is represented by a Gaussian normal distribution (except for profile pairs around the stratopause at noon). The dependence of the O_3 differences on the horizontal distance between the sounding volumes of Aura/MLS and SOMORA is derived. While the mean bias (Aura/MLS – SOMORA) is constant with increasing horizontal distance (up to 800 km), the standard deviation of the O_3 differences increases from around 8 to 12% in the mid-stratosphere. Geographical maps yield azimuthal dependences and horizontal gradients of the O_3 difference field around the SOMORA ground station. Coherent oscillations of O_3 are present in the time series of Aura/MLS and SOMORA (e.g., due to traveling planetary waves). Ground- and space-based measurements often complement one another. We introduce the double differencing technique which allows both the cross-validation of two satellites by means of a ground station and the cross-validation of distant ground stations by means of one satellite. Temporal atmospheric noise in the geographical ozone map over Payerne is significantly reduced by combination of the data from SOMORA and Aura/MLS. These analyses illustrate the synergy between ground-based and space-based measurements.

1 Introduction

The long-term series of O_3 volume mixing ratio profiles recorded by the Stratospheric Ozone Monitoring Radiometer (SOMORA) in Payerne (46.82° N, 6.95° E) since January 2000 forms the basis of the present study which is divided into three main parts.

5 In the first part, the SOMORA data set is utilized for a cross-validation of the satellite experiments Aura/MLS (Froidevaux et al., 2006), ENVISAT/MIPAS (Glatthor et al., 2006; Steck et al., 2006), ENVISAT/GOMOS (Meijer et al., 2004), SAGE-II (Nazaryan et al., 2005), SAGE-III (Polyakov et al., 2005), and UARS/HALOE (Brühl et al., 1996). The references above correspond to previous ozone validation studies of the satellite

10 experiments. In the present study, the vertical O_3 profiles of the satellite limb sounders are compared to coincident profiles of SOMORA. The SOMORA data set has already been involved in numerous cross-validation studies, e.g., Calisesi et al. (2003), Meijer et al. (2004), and Calisesi et al. (2005). All instruments and measurement techniques are briefly described in Sect. 2 while the results of the intercomparison of the various

15 satellite experiments are given in Sect. 3.

In the second part (Sect. 4), a detailed investigation of the spatiotemporal characteristics of the O_3 differences between Aura/MLS (retrieval version 1.5) and SOMORA is performed. The high sampling rate and quality of the ozone profiles collected by the microwave limb sounder on the Aura satellite are crucial for this investigation, which

20 provides information about sensitivity to time and space coincidence criteria. The temporal variation of the stratospheric ozone distribution over Payerne is delineated by the time series of Aura/MLS and SOMORA since August 2004 (start of the Aura/MLS experiment). The comparison of both O_3 time series gives information about the temporal stability of the ground- and space-based microwave radiometers.

25 In the third part, the synergy of ground- and space-based measurements is discussed (Sect. 5). A formalism (double-differencing method) is introduced for cross-validation of non coincident observations in space and time, e.g., two satellite experiments by means of a ground station. The double-differencing method is further tested

for the case of cross-validation of two distant ground stations by use of a satellite. Finally, geographical ozone maps provided by Aura/MLS over central Europe are corrected for atmospheric noise by use of SOMORA's ozone measurements.

2   Instruments and measurement techniques

2.1   The ground-based microwave radiometer SOMORA

The stratospheric ozone monitoring radiometer (SOMORA) monitors the thermal emission of ozone at 142.175 GHz. SOMORA has been developed at the Institute of Applied Physics, University of Bern. The broadband and narrowband acousto-optical spectrometers of SOMORA have 1024 and 2048 channels distributed over a bandwidth of 1 GHz and 50 MHz respectively (Calisesi, 2003). The noise of the brightness temperature (spectrum intensity) is around 0.5 K after an integration time of 30 min. The instrument was first put into operation on 1 January 2000 and was operated in Bern (46.95° N, 7.44° E) until May 2002. In June 2002, the instrument was moved to Payerne (46.82° N, 6.95° E) where its operation has been taken over by MeteoSwiss. SOMORA contributes primary data to the Network for the Detection of Atmospheric Composition Change (NDACC).

The vertical distribution of ozone is retrieved from the recorded pressure-broadened ozone emission spectra by means of the optimal estimation method (Rodgers, 1976). The SOMORA data analysis determines the O_3 volume mixing ratio with less than 20% a priori contribution in the 25 to 55 km altitude range, with a vertical resolution of 8–10 km, and a time resolution of 30 min (sampling time of retrieved profiles). The altitude step of the vertical retrieval grid is around 2.5 km. More details concerning the instrument design, data retrieval, and intercomparison can be found in Calisesi (2000) and Calisesi (2003).

2.2 Satellite limb sounders

The satellite experiments employ the limb sounding technique and provide O_3 profiles with a vertical resolution of 1–3 km. The main characteristics of the satellite experiments are described in Table 1. The measurement techniques can be divided into two groups: (1) measurement of the thermal emission of O_3 as performed by Aura/MLS and ENVISAT/MIPAS at different wavelengths, (2) measurement of ozone absorption features in spectra of the Sun and stars rising or setting at the Earth's horizon (occultation technique). The atmospheric emission sounders require a precise calibration of the receivers. A usefulness of this technique is the relative high data rate compared to the solar occultation technique providing only two O_3 profiles per orbit revolution of the satellite. ENVISAT/GOMOS observes around 40–50 star occultations per orbit revolution, but at the moment, star occultations on the dayside are not usable for accurate O_3 profiling because of stray light from the Sun (Meijer et al., 2004). One advantage of the occultation technique is its self-calibrating nature, since the spectrum of the star or Sun is always measured with ray paths outside and inside the Earth's atmosphere. All selected measurement techniques require sophisticated optical systems, precise pointing, sensitive receivers, and advanced retrieval techniques. The measurement accuracy has to be regularly controlled by cross-validation studies.

3 Cross-validation of satellite limb sounders by SOMORA

Since the vertical resolution of the satellite limb sounders is better than the resolution of SOMORA, averaging kernel smoothing is applied to the ozone profiles of all satellite data

$$X_{\text{sat,low}} = X_{\text{apriori,ground}} + \mathbf{A}_{\text{ground}} \left(X_{\text{sat,high}} - X_{\text{apriori,ground}} \right) . \tag{1}$$

$\mathbf{A}_{\text{ground}}$ is the averaging kernel matrix of the ground-based microwave radiometer, and $X_{\text{apriori,ground}}$ is the a priori profile for the inversion of the ground-based measurement.

$X_{sat,low}$ is the smoothed profile of the satellite measurement, adjusted to the vertical resolution of the ground-based measurement. The relative difference profile ΔX_r is given by

$$\Delta X_r = \frac{X_{sat,low} - X_{ground}}{X_{ground}}. \tag{2}$$

The application of averaging kernel smoothing for the comparison of profiles with different altitude resolutions has been introduced and described by Tsou et al. (1995). A positive effect is that the influence of $X_{apriori,ground}$ is largely removed by subtraction of $X_{sat,low}$ and X_{ground}. On the other hand, the a priori and the averaging kernels of the satellite profiles are not considered by Eq. (1). At the moment, it would be too much effort to gather all a priori profiles and averaging kernel matrices of the satellite missions. However Calisesi et al. (2005) have already derived the extensive equations for this complete case of comparison and applied it to a cross-validation of SOMORA and the ERS-2/GOME experiment. The ozone measurements of GOME have a mean positive deviation of around 2–9% in the altitude range h=25–55 km with respect to SOMORA (this result agrees with the cross-validations in the following).

Each selected profile pair should be coincident in space and time. Spatial coincidence of the ground- and space-based measurements is chosen here to be satisfied when the sounding volumes of the satellite and the ground station have a horizontal distance $d < 800$ km. Time coincidence shall be given when both measurements are within 1 h. Since SOMORA's O_3 profiles are continuously obtained with a sampling rate of 30 min, the fulfillment of the time coincidence criterion is no problem at all.

The arithmetic averages of the relative difference profiles of Aura/MLS, ENVISAT/MIPAS, ENVISAT/GOMOS, SAGE-II, SAGE-III, and UARS/HALOE are shown in Fig. 1 with respect to the ground station SOMORA. The number of profile pairs is given in the figure legend. Aura/MLS, ENVISAT/MIPAS, ENVISAT/GOMOS, SAGE-II, SAGE-III, and UARS/HALOE have relative differences within 10% at altitudes below 45 km. The standard deviations of the relative differences are typically around 10%. Beyond

[ACPD](#)

7, 5053–5098, 2007

Comparison and synergy of stratospheric ozone measurements

K. Hocke et al.

Title Page

Abstract | Introduction

Conclusions | References

Tables | Figures

|◄ | ►|

◄ | ►

Back | Close

Full Screen / Esc

Printer-friendly Version

Interactive Discussion

EGU

45 km altitude, the solar occultation experiments SAGE-II and SAGE-III observe higher ozone values than the atmospheric emission sounders SOMORA, ENVISAT/MIPAS, and Aura/MLS. The star occultation experiment ENVISAT/GOMOS measures lower ozone values at upper altitudes compared to the other instruments. A long-term cross-validation of ENVISAT/GOMOS and MIPAS ozone profiles with ground-based lidar measurements of O_3 gave similar results (Meijer et al., 2006). A negative bias of –5% is found for GOMOS at h=45 km, while the MIPAS ozone profiles (ESA operational retrieval version IPF 4.61 and 4.62) have a positive bias of around 5% at h=20 km and h=35–45 km relative to the lidar profiles. Kyrölä et al. (2006) show that GOMOS provides a higher precision at upper altitudes if only the bright star occultations are selected.

The reason for the increase of the relative deviations at upper altitudes may partly be due to the decrease of the ozone concentration with increasing height. Another reason might be the occurrence of horizontal gradients in the ozone distribution beyond 45 km where photo dissociation yields low ozone values after sunrise and high ozone values after sunset. In case of the solar occultation experiments, the retrieval of the ozone profiles is more sophisticated at altitudes beyond 45 km since the assumption of spherical symmetry of the atmosphere is not valid at these altitudes in the solar terminator region.

Good agreement (<10%) is found among the satellite limb sounders SAGE-II, Aura/MLS, and UARS/HALOE at all altitudes from 25 to 60 km. Nazaryan et al. (2005) report a positive bias of around 5% for SAGE-II (version 6.1) with respect to HALOE (version 19) at altitudes from 20 to 50 km. This finding is fairly consistent with our study (Fig. 1).

Application of the averaging kernel smoothing method for a cross-validation has a a serious limitation since the method gives no information about the vertical, small-scale oscillations of the satellite profiles. These fluctuations can be due to instabilities of the retrieval algorithms. The simplest way to perform cross-validation is by subtracting the

original profiles of satellite and ground station

$$\Delta X_{r,\text{simple}} = \frac{X_{\text{sat,high}} - X_{\text{ground}}}{X_{\text{ground}}}. \tag{3}$$

The simple difference profiles give information about a possible occurrence of systematic, high-frequency oscillations in the satellite profiles. The arithmetic averages of these difference profiles are shown in Fig. 2. Fortunately, the results of Figs. 2 and 1 are quite similar. Thus, systematic effects of high-frequency oscillations of the selected satellite experiments seem to play a minor role. Figure 2 also shows that the simple method of cross-validation is suitable for SOMORA, since SOMORA measures a high-resolution spectrum with a high accuracy (error of the brightness temperature is around 0.5 K). This yields a good vertical resolution (8–10 km) and a small contribution of the a priori profile (<20%), so that the impact of averaging kernel smoothing is relatively small on cross-validations with SOMORA.

4 A detailed comparison of Aura/MLS and SOMORA

The microwave limb sounder on the Aura satellite provides high quality ozone profiles with a sampling time of 25 s. For the SOMORA radiometer at Payerne, we find about 5000 coincident profile pairs from August 2004 to June 2006. This is 20 times or more than we found for the other satellite limb sounders. The huge amount of coincident profile pairs of Aura/MLS and SOMORA allows a statistical study of the distributions and of the characteristics of the O_3 differences.

The Aura orbit is sun-synchronous with 98° inclination, 01:45 p.m. ascendig (north-going) equator-crossing (Waters et al., 2006). At northern mid-latitudes the Aura over-pass times are roughly around noon and midnight. Hence the ensemble of O_3 difference profiles can be divided into a noon and midnight part. In the upper stratosphere this separation is meaningful, since the O_3 volume mixing ratio is smaller during daytime and larger during nighttime.

Comparison and synergy of stratospheric ozone measurements

K. Hocke et al.

EGU

For an overview of the coincident O_3 VMR measurements of Aura/MLS and SOMORA, the scatter plots are shown in Fig. 3 at altitudes h=27, 32, 37, 40, 46, and 52 km around noon. The linear regression line of the observations (black line) agrees well with the red line which indicates the case of identity of both data sets. The scatter plots of the measurements around midnight (not shown) are quite similar to Fig. 3 but at h=52 km the black line shows a positive bias with respect to the red line. If the scatter plot is performed for all measurements (day and night) of SOMORA and Aura/MLS at h=52 km, an almost perfect agreement of the black and red line is obtained since the negative bias at noon compensates for the positive bias at midnight. Thus a separate analysis of the noon and midnight ozone measurements is required at altitudes beyond 50 km.

4.1 Probability density function of the O_3 differences

The derivation of the mean differences and standard deviations in the previous Sect. 3 implicitly assumed a Gaussian normal distribution of the O_3 differences. We check this assumption for the noon and midnight ensembles of the profile pairs Aura/MLS-SOMORA (horizontal distance <800 km and time difference <1 h).

The probability density function of the midnight ensemble is shown as black area in Fig. 4 at altitudes h=27, 32, 37, 40, 46, and 52 km. The red line indicates the best fit of the Gaussian normal distribution to the observed distribution of O_3 differences. The yellow horizontal line is two times the standard deviation σ, while the green line denotes the mean average (bias) of the Gauss curve. At most altitudes, the observed distributions are well represented by a Gaussian normal distribution.

The results for the noon ensemble are shown in Fig. 5. It is obvious that the agreement between the Gauss curve and the observed distribution is significantly weaker at altitudes 46 and 52 km. At 52 km a few O_3 differences (values >50%) drag the fitted Gauss curve to the right-hand-side. The reason for the few profile pairs with large positive deviations has not yet been determined. Possibly it is a failure of the quality control of the SOMORA retrieval at upper altitudes. The mean bias at h=52 km may be

reduced from around 15 to 10%, if the few large deviations are ignored (Fig. 5). Generally, the assumption of a Gaussian normal distribution is justified for the O_3 differences of Aura/MLS and SOMORA.

4.2 Dependence of the O_3 differences on the horizontal distance

Spatial coincidence of two stratospheric measurements are not uniformly defined in validation studies. In the literature, collocation of two stratospheric measurements is fulfilled when the horizontal distance of the sounding volumes is <400, ..., 800 km (Calisesi et al., 2005; Meijer et al., 2004). Alternatively, limits of latitude and longitude have been used, e.g., ±5° for the latitude difference and ±15° for the longitude difference between the satellite sounding volume and the ground station (Dumitru et al., 2006).

The data sets of Aura/MLS and SOMORA are appropriate to investigate the spatial coincidence criterion in more detail. The complete ensemble consists of 5121 coincident profile pairs (horizontal distance <800 km, Δt<1 h) observed from August 2004 to June 2006. The relative O_3 differences (Aura/MLS - SOMORA, blue dots) are shown as a function of the horizontal distance in Fig. 6 for the selected altitudes from 27 to 52 km. The mean (red line) and the standard deviation (green line) of subsets of 50 profile pairs are calculated as function of horizontal distance. A significant dependence of the mean on the horizontal distance is not obvious, as the mean seems to be constant with increasing horizontal distance. For a mid-latitude station such as SOMORA in Payerne, this result is not surprising. An increase or decrease of the mean O_3 difference with increase of horizontal distance would imply a minimum or maximum in the mid-latitude ozone distribution at the location of the ground station. Certainly this is not the case for measurements of a long time interval. The standard deviation increases slightly with increasing horizontal distance, e.g., at h=32 km the standard deviation increases from around 8 to 12% (green line in Fig. 6). This increase is possibly due to horizontal gradients in the ozone distribution over Payerne, or to larger scatter associated with larger spatial differences between the measurements.

In summary, the selection of the spatial collocation criterion seems to be unproblematic at mid-latitudes. For the derivation of mean difference profiles it does not matter if the horizontal distance limit is set to 400 or 800 km. The standard deviation is sensitive to the horizontal distance but a larger amount of profile pairs compensates for the disadvantage of a higher standard deviation with increase of horizontal distance.

4.3 Dependence of the O_3 differences on the time distance

Time coincidence is defined in the present study as $\Delta t < 1$ h while other studies accept time differences up to 20 h in the stratosphere (Meijer et al., 2003; Veiga et al., 1995). The comparison of two O_3 measurements separated in time can be heavily biased if temporal ozone fluctuations with time scales from hours to days are present. For illustration of possible effects, the nighttime Aura/MLS O_3 measurements of the time interval 10 January to 20 January are selected. This time interval provides 56 coincident pairs of MLS and SOMORA profiles. Each profile is compared to profiles of SOMORA having time lags from –20 days to +20 days in steps of 4 h. In total, around 13000 difference profiles have been calculated for the short time interval in mid of January. The dependences of the mean bias (red line) and the standard deviation (green line) of the O_3 differences on the time lag Δt of the selected SOMORA measurements with respect to the Aura/MLS measurements are shown in Fig. 7. The crossing of the solid black lines denotes the orientation point where time lag and ΔO_3 are zero.

At altitudes h=27, 37, 40, and 46 km the minimal bias and standard deviation are achieved when Δt is between –2 and +2 days. Surprisingly, the mean bias is most variable in the time lag region –3 to +3 days at h=32 km. At h=52 km, the effect of the diurnal change of ozone is obvious. A 24-h oscillation can be also seen at some other altitudes, e.g., h=40 km. A strong bias is present at a time lag Δt=10 days. The arrival of ozone-rich air possibly explains the negative values of Aura/MLS-SOMORA after 10 days.

The disturbing influence of temporal ozone fluctuations is possibly reduced when longer time intervals are considered. We selected only ten days of Aura/MLS mea-

surements in Fig. 7. The 24-h oscillation should be reduced when noon and midnight profiles of Aura/MLS are put together. Nevertheless, the fulfillment of the condition of time coincidence seems to be more important than the condition of spatial coincidence (though this is bound to vary with season and latitude).

4.4 Geographical maps of the O_3 differences around the SOMORA ground station

In addition to the dependence on the horizontal distance, there may exist a dependence of the O_3 differences on the azimuthal direction of the satellite sounding volume with respect to the location of the ground station. Geographical maps of the O_3 differences around Payerne can illustrate both dependences.

An interpolation procedure of the MATLAB computing and visualization software (version 6) is used for the generation of the geographical maps. The procedure grid-data is based on a Delaunay triangulation as performed by the quickhull algorithm of Barber et al. (1996). The irregularly distributed differences $\Delta O_3(\text{lat}_i, \text{lon}_i)$, $i = 1, ..., n$ are interpolated to a regular grid with a step size of $0.1°$ in latitude and longitude. lat_i and lon_i denote the latitude and longitude coordinate of the satellite sounding volume of the i-th measurement.

The relative O_3 difference maps of the profile pairs around midnight are depicted in Fig. 8. At altitudes h=27, 32, 37, and 40 km a meridional gradient might be present, with positive and negative deviations south and north of Payerne, respectively. Payerne is indicated by the black cross in the middle of the graph. The stripes in the graphs are exactly aligned with the satellite orbit during nighttime (Aura's orbit inclination is $98°$). Around midnight, the satellite overpass track is from NNE to SSW direction while around noon the overpass direction is from SSE to NNW. The change in satellite over-pass direction is obvious when the stripes of Fig. 8 are compared to those of Fig. 10 which shows the geographical maps of the relative O_3 differences around noon.

The occurrence of stripes in the maps might be due to the interplay of several factors. The coordinates of the Aura profiles are not randomly distributed but they are on grid points of a weakly-varying grid having a spacing of around $1.5°$. The spatial sampling

Full Screen / Esc

Printer-friendly Version

Interactive Discussion

EGU

modus of the Aura/MLS profiles, phases of instrument/calibration errors of the ground- and spacebased radiometers, and temporal variations of the ozone distribution (e.g., due to planetary waves, seasonal changes) may produce the stripes in the maps.

4.5 Time series of the O_3 measurements by Aura/MLS and SOMORA

The O_3 time series of Aura/MLS (red line) and SOMORA (blue line) are shown in Fig. 11 for the measurements around midnight. For a correct comparison, averaging kernel smoothing has been applied to the profiles of the Aura/MLS series (Eq. 1). The Aura/MLS and the SOMORA series have been smoothed in time by a moving average over 30 data points corresponding to an interval of 3–4 days. The same analysis has been performed for the ozone measurements around noon which are depicted in Fig. 11. A gap occurs in all time series during summer 2005, since the front end of the SOMORA microwave radiometer was upgraded during this period.

The agreement of the Aura/MLS and SOMORA series depends on both, altitude and time. A positive deviation of the SOMORA series with respect to Aura/MLS occurs after August 2005 at altitudes below 32 km. It is likely that this deviation is somehow connected to the change of the SOMORA frontend in July 2005. Another significant difference of SOMORA and Aura/MLS occurs at h=52 km. The ozone values of Aura/MLS are higher than SOMORA around noon (Fig. 11) and smaller than SOMORA around midnight (Fig. 10). Thus the diurnal amplitude of the ozone variation at h=52 km is smaller for Aura/MLS than for SOMORA.

A remarkable agreement of Aura/MLS and SOMORA is found for the strong, planetary-wave like oscillations in ozone from January to April 2005 at all altitudes from 27 to 52 km. The agreement of the time series of Aura/MLS and SOMORA is excellent at altitudes from 37 to 46 km from August 2004 to June 2006. Seasonal changes and short-term fluctuations (10–30 days) are coherently monitored by both instruments.

4.6 Dependence of the O_3 differences on tropospheric attenuation

The electromagnetic radiation of stratospheric ozone has to travel through the troposphere before the spectral line is recorded by the ground-based microwave radiometer. Particularly tropospheric water vapor attenuates the ozone emission from the stratosphere (Ingold et al., 1998). The forward model of SOMORA's retrieval includes a standard water vapor profile which is scaled by a single multiplication factor. The multiplication factor is estimated by analyzing the observed signal intensity at the wings of the spectral line (Calisesi, 2003). So the effect of tropospheric attenuation is individually considered for each spectrum inversion.

Since the stratospheric limb soundings of Aura/MLS are free of tropospheric attenuation, the O_3 differences (SOMORA – Aura/MLS) can indicate the quality of the so-called tropospheric correction of SOMORA's retrieval. The O_3 differences are shown as function of the tropospheric attenuation in Fig. 12. A clear trend or dependence of the O_3 differences on tropospheric attenuation (or water vapor) is not present. Thus the quality of SOMORA's O_3 profiles seems to be ensured during times of enhanced water vapor amount and signal attenuation in the troposphere.

4.7 Dependence of the O_3 differences on O_3

It could be possible that the systematic error of SOMORA is constant or proportional to the ozone volume mixing ratio. Let us assume that the ozone measurements of Aura/MLS are the truth. Then the differences ΔO_3 between SOMORA and Aura/MLS describe the error of SOMORA

$$O_3 = O_3(\text{Aura})$$
$$\Delta O_3 = O_3(\text{SOMORA}) - O_3(\text{Aura}).$$

Figure 13 depicts all observed differences ΔO_3 (noon and midnight) as function of O_3. The red line is the moving average over 100 data points. In the middle part of each viewgraph O_3 is approximately constant with O_3, and we may conclude that the

systematic error of SOMORA is constant. Figure 13 also shows that ΔO_3 increases when Aura/MLS measures small ozone mixing ratios.

However the systematic error of SOMORA seems to be constant with O_3 for the majority of the observation points in Fig. 13.

4.8 Mean O_3 difference profiles of Aura/MLS and SOMORA

The mean O_3 difference profiles of the whole time interval from the start of the Aura/MLS experiment in August 2004 to June 2006 are depicted in Fig. 14. The left-hand-side panel shows the mean O_3 profiles of Aura/MLS (red) and SOMORA (blue). In addition the mean of the Aura/MLS profiles is shown by the green line when previously the profiles have been smoothed by averaging kernels (Eq. 1).

The mean O_3 relative difference profile (Aura/MLS − SOMORA) is shown by the solid blue line in the middle panel of Fig. 14. The standard deviation is given by the dashed blue line. The yellow band indicates the ±10% area which is the zone of good agreement. Again, the differences between Aura/MLS and SOMORA have been separately calculated for each coincident profile pair. The Aura/MLS profile has been adjusted to the lower vertical resolution of SOMORA by averaging kernel smoothing. The mean difference is <10% at altitudes below 60 km. At altitudes from 30 to 50 km the bias is <5%. The standard deviation is around 10–20%. The mean profile of the absolute differences is shown at the right-hand-side of Fig. 14.

The mean O_3 profiles around noon are depicted in 15. While the mean ozone profiles and the absolut difference profile around noon are quite similar to the results of the midnight ensemble, a large positive deviation (20–30%) occurs in the mean O_3 relative difference profile at h=55–65 km. This is partly due to the decrease of the ozone volume mixing ratio during daytime at these altitudes. In addition we noted in Sect. 4.1 some outliers in the noon ensemble which might be better excluded in future studies.

In summary a thorough validation of the Aura/MLS experiment has been conducted by means of the long-term data set of the SOMORA microwave radiometer in Payerne. The main problem (and working task) seems to be the positive deviation of

the SOMORA ozone measurements at altitudes below 32 km which occurred after the frontend change of the SOMORA radiometer in July 2005. The detailed comparison of Aura/MLS and SOMORA shows the potential of both instruments for measurements of the highly variable, spatiotemporal ozone distribution in the stratosphere and lower mesosphere. Some fundamental questions such as selection of the spatial coincidence criterion, probability density distribution of ozone differences at noon and midnight, and influence of tropospheric attenuation have been clarified. In the following section the synergy of ground- and space-based measurements is addressed.

5 Synergy of ground- and space-based measurements

5.1 Double differencing method for cross-validation of two satellites

In Fig. 1 we compared ozone measurements of 6 satellite limb sounders by means of the long-term data set of the SOMORA microwave radiometer in Payerne. According to Table 1, the data intervals of the satellites are quite different, e.g., the ENVISAT/MIPAS data set already stopped before the launch of the Aura satellite. Furthermore, the local times of the measurements are quite different, e.g., the solar occultation measurements are always at sunrise and sunset while the Aura/MLS measurements are around noon and midnight.

Is it justified to derive the difference of two satellite experiments by taking the difference of their difference profiles (e.g., the difference of the difference profiles in Fig. 1)? This question is of great interest, since non-coincident measurements of satellite experiments could be compared by taking a ground station as reference. For simplicity the differencing of difference profiles shall be named double differencing.

Ideally, double differencing will provide the difference of the systematic errors, $(E_A - E_B)$, of the satellite experiments A and B. This is easily explained in Fig. 16. Double differencing of satellite observations with respect to a ground station removes the contributions of diurnal, seasonal, and interannual composition changes and trends.

Also, a constant bias versus the ground station is removed by taking the difference of the lengths of the red lines in Fig. 16. The algebraic formulation is given by

$$O(X_A(t_1), X_B(t_2)) := \tag{4}$$
$$= [X_A(t_1) - X_G(t_1)] - [X_B(t_2) - X_G(t_2)]$$
$$= [(X_{\text{true}}(t_1) + E_A) - (X_{\text{true}}(t_1) + E_G)] -$$
$$[(X_{\text{true}}(t_2) + E_B) - (X_{\text{true}}(t_2) + E_G)]$$
$$= E_A - E_B.$$

Again, the result of double differencing is equal to the difference of the systematic errors of the satellites, if the systematic error E_G of the ground station is constant (long-term stability of the ground station has to be ensured). The symbol O indicates the double differencing operator. $X_A(t_1)$ is the vertical ozone profile observed by A nearby the ground station at time t_1. $X_{\text{true}}(t_1)$ is the true ozone profile at the ground station at time t_1. Random measurement errors are not considered in Eq. (4) but their influence can be reduced by averaging over time intervals, e.g., measurements of a month or a season.

A dependence of the systematic errors E_A, E_B, and E_G on the ozone profile X and/or other parameters has been neglected in Eq. (4). Analysis of the SOMORA and Aura/MLS data gave no clear relationship between the systematic error and the ozone mixing ratio. Figure 13 seems to favor a constant bias for the ground station SOMORA. Anyway, we should check the case when double differencing is applied to the relative difference profiles and when the systematic errors are proportional to X. For example, $E_G(t) = e_G X_{\text{true}}(t)$ where e_G is the constant, relative systematic error of the ground station. The relative double differencing operator O_r subtracts the relative difference profiles

$$O_r(X_A(t_1), X_B(t_2)) := \tag{5}$$
$$= \frac{[X_A(t_1) - X_G(t_1)]}{X_G(t_1)} - \frac{[X_B(t_2) - X_G(t_2)]}{X_G(t_2)}$$

Comparison and synergy of stratospheric ozone measurements

K. Hocke et al.

EGU

$$= \left[\left(\frac{X_{\text{true}}(t_1)}{X_G(t_1)} + \frac{E_A(t_1)}{X_G(t_1)} \right) - \left(\frac{X_{\text{true}}(t_1)}{X_G(t_1)} + \frac{E_G(t_1)}{X_G(t_1)} \right) \right] -$$

$$\left[\left(\frac{X_{\text{true}}(t_2)}{X_G(t_2)} + \frac{E_B(t_2)}{X_G(t_2)} \right) - \left(\frac{X_{\text{true}}(t_2)}{X_G(t_2)} + \frac{e_G(t_2)}{X_G(t_2)} \right) \right]$$

$$\approx e_A - e_B.$$

For the last step of Eq. (5), we inserted the approximations

$$5 \quad E_A(t) = e_A X_{\text{true}}(t) \approx e_A X_G(t)$$

$$E_B(t) = e_B X_{\text{true}}(t) \approx e_B X_G(t)$$

$$E_G(t) = e_G X_{\text{true}}(t) \approx e_G X_G(t).$$

So, the relative double differencing operator O_r gives the difference of the relative systematic errors of the satellites A and B. In this second case, all relative systematic
10 errors e_A, e_B, and e_G are assumed to be constant. This implies that the systematic errors are proportional to the parameter X (e.g., ozone volume mixing ratio).

The assumption of a constant bias (for Eq. 4) or a constant relative bias (for Eq. 5) should be sufficient for most cross-validation studies. The mean O_3 difference profile (according to Eq. 4) of the non coincident measurements of ENVISAT/MIPAS and
15 Aura/MLS is depicted in Fig. 17 as example for double differencing with respect to the ground station SOMORA.

The critical point of double differencing is the required long-term stability of the ground station over many years. The long-term stability of ground station measurements is crucial for validation of past and present satellite missions and for monitor-
20 ing/detection of long-term trends in the atmospheric composition. Supporting, collecting, and archiving of ground station measurements with long-term stability is the most challenging task of the Network for the Detection of Atmospheric Composition Change (NDACC, http://www.ndacc.org) which was originally founded in 1991 as the Network for the Detection of Stratospheric Change (NDSC).

5.2 Double differencing method for cross-validation of two ground stations

Similarly to the previous subsection, two ground stations at different places can be cross-validated by use of coincident satellite measurements. Contrary to some nadir sounders, the systematic errors of atmospheric limb sounders are possibly indepen-
5 dent of latitude and longitude. Thus a validation of far distant ground stations by one satellite limb sounder is reasonable.

As an example, the microwave radiometer SOMORA is compared with the microwave radiometer on Mauna Loa (Hawaii) for observations from October to December 2005. The Mauna Loa instrument consists of an automated microwave receiver
10 and a 120-channel spectrometer tuned to the ozone transition at 110.836 GHz (Parrish et al., 1992). The ozone profiles of the Mauna Loa microwave radiometer have been carefully validated by intercomparisons with other measurement techniques (e.g., McPeters et al., 1999). The ozone measurements of the satellite experiment Aura/MLS are taken as reference for double differencing. In the same manner as for SOMORA,
15 the coincident and collocated Aura/MLS profiles are adjusted to the vertical resolution of the Mauna Loa radiometer using the averaging kernel matrix and the a priori ozone profile of Mauna Loa's retrieval. These data are available via the ground station segment of the new Aura Validation Data Center (AVDC) of NASA. Since the shape of the O_3 profile is quite different over Mauna Loa and Payerne, the relative double
20 differencing operator O_r (Eq. 5) has been favored.

The left-hand-side of Fig. 18 shows the mean difference profile Aura/MLS-Mauna Loa calculated from 160 coincident profile pairs (selection criteria: horizontal distance <800 km and Δt<3 h, since Mauna Loa's ozone profiles have an integration time of around 4 h). The middle panel shows the mean difference profile Aura/MLS-SOMORA
25 for 803 coincident pairs. The right-hand-side gives the difference Mauna Loa-SOMORA which is equal to the double difference (Aura/MLS-SOMORA) − (Aura/MLS-Mauna Loa). A good agreement (<5%) is found between Aura/MLS and Mauna Loa at lower altitudes (<35 km) and at upper altitudes (>50 km). Thus the higher deviations between

Aura/MLS and SOMORA at these altitude ranges seem to be due to shortcomings of the SOMORA radiometer. This is in agreement to our considerations in Sect. 4. A deviation of around −9% is found between Aura/MLS (retrieval version 1.5) and the Mauna Loa radiometer at altitudes around 40 km. The upcoming retrieval version 2.2

5 of Aura/MLS is expected to diminish this bias. The example shows that cross-validation of ground stations by satellite limb sounders may provide more clarity about the states of the ground stations and the satellites.

5.3   Combination of Aura/MLS and SOMORA measurements for ozone maps

Geographical maps of the O_3 differences have been derived in Sect. 4.4, and horizontal

10 gradients of the ozone distribution became partly visible in these maps. Here we derive geographical maps of the mean ozone field around Payerne during January–March 2005 when a strong planetary-wave like oscillation is present in the ozone distribution (see ozone time series of Fig. 10). Averaging of ozone fields over 1–3 months is of interest since stationary phenomena may be revealed (e.g., impact of upward orographic

15 wave flux).

The continuous ground-based measurements of SOMORA allow the accurate determination of the mean ozone profile (<SOMORA>: average of all SOMORA profiles within the selected time interval). The horizontal spatial information is contained in the Aura/MLS profiles and as described in Sect. 4.4 we can derive a mean differ-

20 ence field <Aura/MLS-SOMORA> by subtraction of coincident profiles of Aura/MLS and SOMORA and relating these differences to the geographic positions of the satellite sounding volumes. If we add <SOMORA> to the difference field, an absolute ozone map around Payerne is generated. The right-hand-side of Fig. 19 shows these ozone maps at h=27 km and h=32 km, representing a combination of satellite- and ground-

25 based measurements.

Pure satellite ozone maps are shown on the left-hand-side of Fig. 19 for comparison. These maps are solely based on the Aura/MLS measurements (averaging kernel smoothing has been applied to the profiles for reduction of the noise due to the higher

vertical resolution of Aura/MLS). However these ozone maps still contain noise which is possibly due to traveling planetary waves and other short-term atmospheric fluctuations. These temporal fluctuations are reduced in the ozone maps on the right-hand-side since the coincident measurements of SOMORA are taken as reference for the Aura/MLS profiles. It can be that a more sophisticated analysis of the satellite data may reduce the noise too (e.g., subtraction of a mean from each swath of satellite measurements). On the other hand, the position of the ground station in the center of the map should be the best reference point for determination of horizontal gradients.

A meridional gradient is visible in the ozone maps. The ozone values in the south of Payerne are around 1 ppm higher than in the north of Payerne. Breaking planetary waves transport ozone-rich air from the south and ozone-poor air from the north into the mid-latitude stratosphere during winter (Calisesi et al., 2001). Thus the meridional gradient in Fig. 19 is reasonable.

6 Conclusions

The cross-validation study of stratospheric ozone profiles gave the main result that the various instruments and measurement techniques agree within 10% at altitudes below 45 km (Fig. 1). At altitudes 45–60 km, the relative O_3 differences are within a range of 50%. Larger deviations at upper altitudes are attributed in part to larger relative measurement errors caused by lower O_3 concentrations. A cross-validation study is always a snapshot, particularly the upcoming retrieval version 2.2 of Aura/MLS is expected to come closer to SAGE-II.

The detailed statistical study of about 5000 O_3 differences of Aura/MLS (retrieval version 1.5) and SOMORA gave the following results: (1) The O_3 differences are well represented by a Gaussian normal distribution (Fig. 4). (2) The mean O_3 difference profile does not depend much on the limit for spatial coincidence of the ground- and satellite-based measurements (Fig. 6). This result is probably always valid when no persistent extremum of the horizontal ozone distribution over the ground station is present. (3)

The standard deviation of the O_3 differences increases slightly with increase of horizontal distance (e.g., from 8 to 12% at h=32 km while the horizontal distance is increased from 0 to 800 km). (4) The mean bias and the standard deviation can strongly depend on the time lag between the ground-based and space-based measurements (Fig. 7).

5 (5) The geographical maps of the mean $\Delta O_3/O_3$ fields around the SOMORA radiometer at Payerne show stripes aligned with the orbit of the Aura satellite (Fig. 8). The stripes could be a signature of measurement inaccuracies of SOMORA and Aura/MLS such as calibration offsets. Temporal changes of the ozone distribution may also lead to a temporal variation of the relative O_3 differences of SOMORA and Aura/MLS which

10 may produce stripes in the maps. (6) The temporal fluctuations (scales from 10 days to year) in the ozone time series of SOMORA and Aura/MLS over Payerne are coherent in amplitude and phase (Fig. 10). A positive offset of the absolute O_3 VMR measurement is present in the SOMORA observations below h=32 km after August 2005. This offset is probably due to the change of SOMORA's frontend in July 2005 (a reprocessing of

15 SOMORA's data since July 2005 is in work). (7) A dependence of SOMORA's O_3 retrieval result on the amount of tropospheric water vapor is not present (Fig. 12). (8) A dependence of the systematic error of SOMORA on O_3 is not present for the majority of observations (Fig. 13). (9) The mean O_3 difference profile Aura/MLS-SOMORA is within 5% at altitudes from 30 to 50 km (Fig. 14).

20 We emphasized the synergy of ground- and spacebased measurements for cross-validation and described the double differencing method (Eq. 4). It was clarified that double differencing requires long-term stability of the ground station. A constant bias of the ground station plays no role for the accuracy of cross-validation of satellite experiments. An example has been shown where the mean O_3 difference profile of (non coin-

25 cident) ENVISAT/MIPAS and Aura/MLS measurements is derived by taking SOMORA as reference (Fig. 17).

The double differencing method has been utilized for the cross-validation of SOMORA with the Mauna Loa microwave radiometer by using Aura/MLS data (Fig. 18). Modern databases such as NASA's Aura Validation Data Center (AVDC) provide

Comparison and synergy of stratospheric ozone measurements

K. Hocke et al.

EGU

ground- and spacebased measurement data containing all relevant informations required for cross-validation studies and application of the double differencing method (e.g., averaging kernel matrix and a priori of the ground station instrument). Such databases are invaluable for the control of the measurement accuracy and long-term stability of ground- and spacebased instruments.

Another aspect of the synergy of ground- and spacebased measurements is the derivation of stationary ozone fields with high horizontal resolution. An example has been shown where temporal noise in the ozone maps of Aura/MLS is removed by means of the ground station measurements of the SOMORA radiometer (right-hand-side of Fig. 19). A meridional gradient is found in the mean ozone distribution of the stratosphere over central Europe during winter conditions and high planetary wave activity.

References

Barber, C. B., Dobkin, D. P., and Huhdanpaa, H. T.: The quickhull algorithm for convex hulls, ACM Transactions on Mathematical Software, 22, 469–483, 1996. 5064

Brühl, C., Drayson, S. R., Russell III, J. M., Crutzen, P. J., McInerney, J. M., Purcell, P. N., Claude, H., Gernandt, H., McGee, T. J., McDermid, I. S., and Gunson, M. R.: Halogen Occultation Experiment ozone channel validation, J. Geophys. Res., 101, 10 217–10 240, 1996. 5055

Calisesi, Y.: Monitoring of stratospheric and mesospheric ozone with a ground-based microwave radiometer: data retrieval, analysis, and applications, Ph.D. thesis, http://www.iap.unibe.ch/publications/, Philosophisch-Naturwissenschaftliche Fakultät, Universität Bern, Bern, Switzerland, 2000. 5056

Calisesi, Y.: The Stratospheric Ozone Monitoring Radiometer SOMORA: NDSC Application

Document, IAP Research Report 2003-11, http://www.iap.unibe.ch/publications/, Institut für angewandte Physik, Universität Bern, Bern, Switzerland, 2003. 5056, 5066

Calisesi, Y., Wernli, H., and Kämpfer, N.: Midstratospheric ozone variability over Bern related to planetary wave activity during the winters 1994-1995 to 1998-1999, J. Geophys. Res., 106, 7903–7916, 2001. 5073

Calisesi, Y., Stübi, R., Kämpfer, N., and Viatte, P.: Investigation of systematic uncertainties in Brewer-Mast ozone soundings using observations from a ground-based microwave radiometer, Journal of Atmospheric and Oceanic Technology, 20, 1543–1551, 2003. 5055

Calisesi, Y., Soebijanta, V. T., and van Oss, R. O.: Regridding of remote soundings: Formulation and application to ozone profile comparison, J. Geophys. Res., 110, D23306, doi:10.1029/2005JD006122, 2005. 5055, 5058, 5062

Dumitru, M. C., Hocke, K., Kämpfer, N., and Calisesi, Y.: Comparison and validation studies related to ground-based microwave observations of ozone in the stratosphere and mesosphere, J. Atmos. Sol. Terr. Phys., 68, 745–756, 2006. 5062

Froidevaux, L., Livesey, N. J., Read, W. G., Jiang, Y. B., Jimenez, C. C., Filipiak, M. J., Schwartz, M. J., Santee, M. L., Pumphrey, H. C., Jiang, J. H., Wu, D. L., Manney, G. L., Drouin, B. J., Waters, J. W., Fetzer, E. J., Bernath, P. F., Boone, C. D., Walker, K. A., Jucks, K. W., Toon, G. C., Margitan, J. J., Sen, B., Webster, C. R., Christensen, L. E., Elkins, J. W., Atlas, E., Lueb, R. A., and Hendershot, R.: Early validation analyses of atmospheric profiles from EOS MLS on the Aura satellite, IEEE Trans. Geosci. Remote Sens., 44, 1106–1121, 2006. 5055

Glatthor, N., von Clarmann, T., Fischer, H., Funke, B., Gil-López, S., Grabowski, U., Höpfner, M., Kellmann, S., Linden, A., López-Puertas, M., Mengistu Tsidu, G., Milz, M., Steck, T., Stiller, G. P., and Wang, D. Y.: Retrieval of stratospheric ozone profiles from MIPAS/ENVISAT limb emission spectra: a sensitivity study, Atmos. Chem. Phys., 6, 2767–2781, 2006, http://www.atmos-chem-phys.net/6/2767/2006/. 5055, 5079

Ingold, T., Peter, R., and Kämpfer, N.: Weighted mean tropospheric temperature and transmittance determination at millimeter-wave frequencies for ground-based applications, Radio Science, 33, 905–918, 1998. 5066

Kyrölä, E., Tamminen, J., Leppelmeier, G. W., Sofieva, V., Hassinen, S., Seppälä, A., Verronen, P. T., Bertaux, J. L., Hauchecorne, A., Dalaudier, F., Fussen, D., Vanhellemont, F., d'Andon, O. F., Barrot, G., Mangin, A., Theodore, B., Guirlet, M., Koopman, R., Saavedra, L., Snoeeij, P., Fehr, T., Meijer, Y., and Fraisse, R.: Nighttime ozone profiles in the stratosphere and mesosphere by the Global Ozone Monitoring by Occultation of Stars on Envisat, J. Geophys.

Comparison and synergy of stratospheric ozone measurements

K. Hocke et al.

Title Page

Abstract | Introduction

Conclusions | References

Tables | Figures

⏮ | ⏭

◀ | ▶

Back | Close

Full Screen / Esc

Printer-friendly Version

Interactive Discussion

EGU

Res., 111, D24306, doi:10.1029/2006JD007193, 2006. 5059

McPeters, R. D., Hofmann, D. J., Clark, M., Flynn, L., Froidevaux, L., Gross, M., Johnson, B., Koenig, G., Liu, X., McDermid, S., McGee, T., Murcray, F., Newchurch, M. J., Oltmans, S., Parrish, A., Schnell, R., Singh, U., Tsou, J. J., Walsh, T., and Zawodny, J. M.: Results from the 1995 stratospheric ozone profile intercomparison at Mauna Loa, J. Geophys. Res., 104, 30 505–30 514, 1999. 5071

Meijer, Y., Van Oss, A., Swart, D., Kelder, H., and Johnston, P.: Global ozone monitoring experiment ozone profile characterization using interpretation tools and lidar measurements for intercomparison, J. Geophys. Res., 108, 4723, doi:10.1029/2003JD003498, 2003. 5063

Meijer, Y., Baray, J.-L., Bodeker, G., Claude, H., Fricke, K., von der Gathen, P., Godin-Beekmann, S., Hansen, G., Keckhut, P., Leblanc, T., Lolkema, D., McDermid, I., Nakane, H., Pal, S., Snoeij, P., and Swart, D.: Long-term validation of GOMOS, MIPAS and SCIAMACHY ozone and temperature profiles by the ENVISAT quality assessment with lidar (EQUAL) project, Proceedings of the ESA Atmospheric Science Conference, Frascati, Italy, 2006. 5059

Meijer, Y. J., Swart, D. P., Allaart, M., Andersen, S. B., Bodeker, G., Boyd, I., Braathen, G., Calisesi, Y., Claude, H., Dorokov, V., van der Gathen, P., Gil, M., Godin-Beekmann, S., Goutail, F., Hansen, G., Karpetchko, A., Keckhut, P., Kelder, H. M., Koelemeijer, R., Kois, B., Koopman, R. M., Kopp, G., Lambert, J. C., Leblanc, T., McDermid, I. S., Pal, S., Schets, H., Stubi, R., Suortti, T., Visconti, G., and Yela, M.: Pole-to-pole validation of Envisat GOMOS ozone profiles using data from ground-based and balloon sonde measurements, J. Geophys. Res., 109, D23305, doi:10.1029/2004JD004834, 2004. 5055, 5057, 5062

Nazaryan, H., McCormick, M. P., and Russell III, J. M.: New studies of SAGE II and HALOE ozone profile and long-term change comparisons, J. Geophys. Res., 110, D09305, doi:10.1029/2004JD005425, 2005. 5055, 5059

Parrish, A., Connor, B. J., Tsou, J. J., McDermid, I. S., and Chu, W. P.: Ground-based microwave monitoring of stratospheric ozone, J. Geophys. Res., 97, 2541–2546, 1992. 5071

Polyakov, A. V., Timofeyev, Y. M., Ionov, D. V., Virolainen, Y. A., Steele, H. M., and Newchurch, M. J.: Retrieval of ozone and nitrogen dioxide concentrations from Stratospheric Aerosol and Gas Experiment III (SAGE III) measurements using a new algorithm, J. Geophys. Res., 110, D06303, doi:10.1029/2004JD005060, 2005. 5055, 5079

Rodgers, C. D.: Retrieval of atmospheric temperature and composition from remote measurements of thermal radiation, Rev. Geophys. Space Phys., 14, 609–624, 1976. 5056

Comparison and synergy of stratospheric ozone measurements

K. Hocke et al.

Title Page

Abstract | Introduction

Conclusions | References

Tables | Figures

◀ | ▶|

◀ | ▶

Back | Close

Full Screen / Esc

Printer-friendly Version

Interactive Discussion

EGU

Steck, T., Blumenstock, T., von Clarmann, T., Glatthor, N., Grabowski, U., Hase, F., Hochschild, G., Höpfner, M., Kellmann, S., Kiefer, M., Kopp, G., Linden, A., Milz, M., Oelhaf, H., stiller, G. P., Wetzel, G., g. Zhang, Fischer, H., funke, B., Wang, D. Y., von der Gathen, P., Hansen, G., Stebel, K., Kyrö, E., Allaart, M., Marrero, A. R., Remsberg, E., Russel III, J., Steinbrecht, W., Yela, M., and Raffalski, U.: Bias determination and precision validation of ozone profiles from MIPAS-Envisat retrieved with the IMK-IAA processor, Atmos. Chem. Phys. Discuss., 7, 4427–4480, 2007,
http://www.atmos-chem-phys-discuss.net/7/4427/2007/. 5055

Tsou, J. J., Connor, B. J., Parrish, A., McDermid, I. S., and Chu, W. P.: Ground-based microwave monitoring of middle atmosphere ozone: Comparison to lidar and Stratospheric and Gas Experiment II satellite observations, J. Geophys. Res., 100, 3005–3016, 1995. 5058

Veiga, R., Cunnold, D., Chu, W., and McCormick, M.: Stratospheric aerosol and gas experiment I and II comparisons with ozonesondes, J. Geophys. Res., 100, 9073–9090, 1995. 5063

Waters, J. W., Froidevaux, L., Harwood, R. S., Jarnot, R. F., Pickett, H. M., Read, W. G., Siegel, P. H., Cofield, R. E., Filipiak, M. J., Flower, D. A., Holden, J. R., Lau, G. K., Livesey, N. J., Manney, G. L., Pumphrey, H. C., Santee, M. L., Wu, D. L., Cuddy, D. T., Lay, R. R., Loo, M. S., Perun, V. S., Schwartz, M. J., Stek, P. C., Thurstans, R. P., Boyles, M. A., Chandra, K. M., Chavez, M. C., Gun-Shing, C., Chudasama, B. V., Dodge, R., Fuller, R. A., Girard, M. A., Jiang, J. H., Jiang, Y., Knosp, B. W., LaBelle, R. C., Lam, J. C., Lee, K. A., Miller, D., Oswald, J. E., Patel, N. C., Pukala, D. M., Quintero, O., Scaff, D. M., Van Snyder, W., Tope, M. C., Wagner, P. A., and Walch, M. J.: The earth observing system microwave limb sounder (EOS MLS) on the Aura satellite, IEEE Trans. Geosci. Remote Sens., 44, 1075–1092, 2006. 5060

Title Page

Abstract | Introduction

Conclusions | References

Tables | Figures

|◄ | ►|

◄ | ►

Back | Close

Full Screen / Esc

Printer-friendly Version

Interactive Discussion

Table 1. Characteristics of the satellite limb sounders.

Satellite Experiment[1]	Orbit	Data interval[2]	Observation principle	Frequency range	Altitude range	Resolution Δh, Δt	Retrieval version
Aura MLS	$i = 98°$ $h = 705$ km	Aug2004– Jun2006	limb emission	190, 240 GHz	15–60 km	3 km 25 s[3]	v01.51 v01.52
ENVISAT MIPAS	$i = 98.5°$ $h = 800$ km	Aug2002– Mar2004	limb emission	infrared	15–60 km	3 km 80 s[3]	V3o-O3-08[4]
ENVISAT GOMOS	$i = 98.5°$ $h = 800$ km	Oct2002– Dec2005	star occultation	UV-VIS-NIR[5]	15–60 km	3 km 120 s[3]	GOPR 6.0cf
ERBS SAGE-II	$i = 57°$ $h = 650$ km	Oct2002– Feb2005	solar occultation	UV-VIS[5]	20–60 km	1.5–2 km <2–3 min[6]	v6.2
Meteor-3M SAGE-III	$i = 99.6°$ $h = 1000$ km	May2003– Aug2003	solar occultation	UV-VIS[5]	20–60 km	1.5–2 km <2–3 min[5]	Polyakov et al. (2005) v3
UARS HALOE	$i = 57°$ $h = 580$ km	Sep2002– Nov2005	solar occultation	infrared	20–80 km	1.6 km <2–3 min[6]	V19

[1] Acronyms of experiments: Microwave Limb Sounder (MLS), Michelson Interferometer for Passive Atmospheric Sounding (MIPAS), Global Ozone Monitoring by Occultation of Stars (GOMOS), Stratospheric Aerosol and Gas Experiment (SAGE), Halogen Occultation Experiment (HALOE).

[2] The present validation study is based on data from this time interval. Operation of Aura and ENVISAT is going on.

[3] Average sampling time of profiles.

[4] Retrieval of IMK FZ Karlsruhe (Glatthor et al., 2006).

[5] UV: ultraviolet, VIS: visible, NIR: near infrared, electromagnetic radiation.

[6] This is the measurement time of a vertical profile.

The sampling time of profiles is around (orbit revolution time/2).
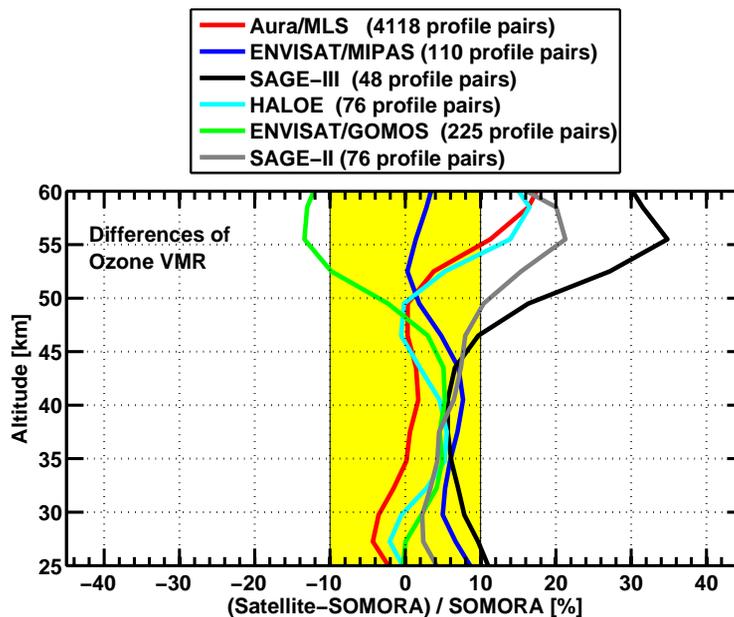
Fig. 1. Mean differences of the observed O_3 volume mixing ratios of satellite limb sounders with respect to the ground station SOMORA in Payerne. Averaging kernel smoothing (Eq. 1) has been applied.

EGU
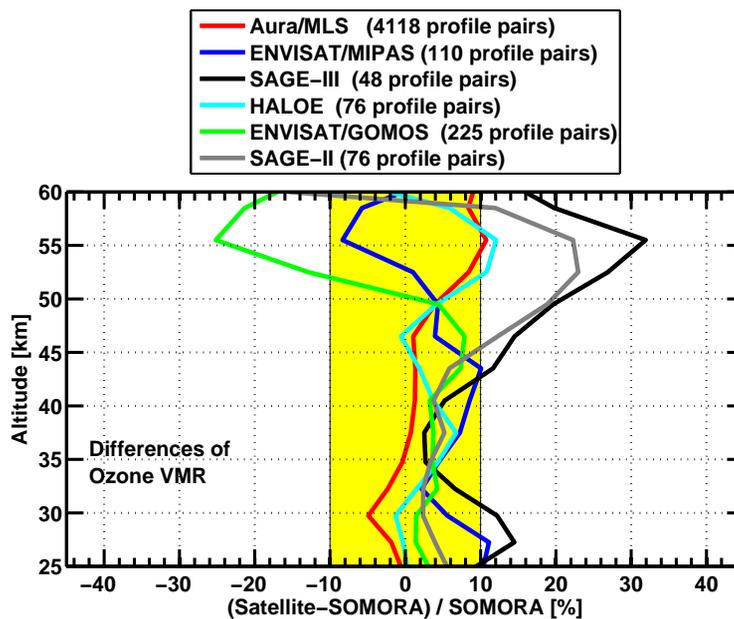
Fig. 2. Similar as Fig. 1 but without averaging kernel smoothing of the satellite profiles.

ACPD

7, 5053–5098, 2007

Comparison and synergy of stratospheric ozone measurements

K. Hocke et al.

Title Page

Abstract | Introduction

Conclusions | References

Tables | Figures

◄ | ►►

◄ | ►

Back | Close

Full Screen / Esc

Printer-friendly Version

Interactive Discussion

EGU
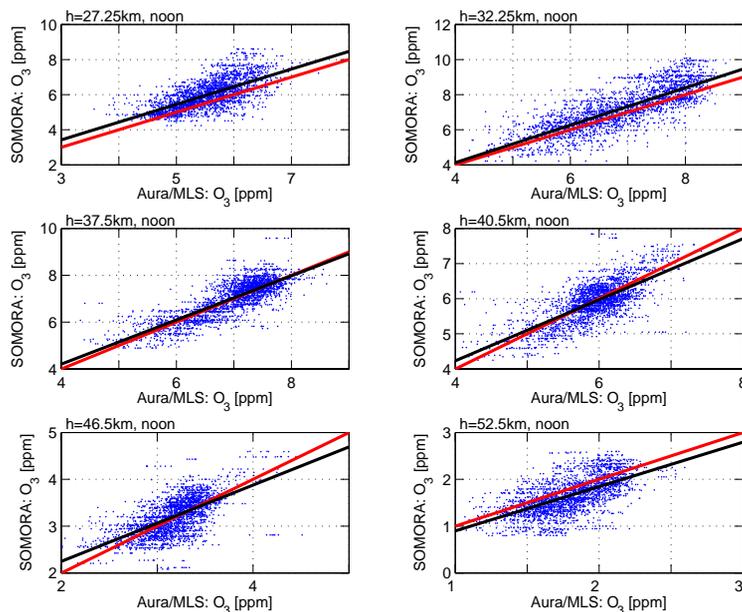
Fig. 3. Scatter plots of coincident O_3 VMR measurements of Aura/MLS and SOMORA at altitudes 27, 32, 37, 40, 46, and 52 km around noon. The black line is the best fit straight line, while the red line would be obtained for a perfect agreement (O_3(SOMORA)=O_3(Aura/MLS)).
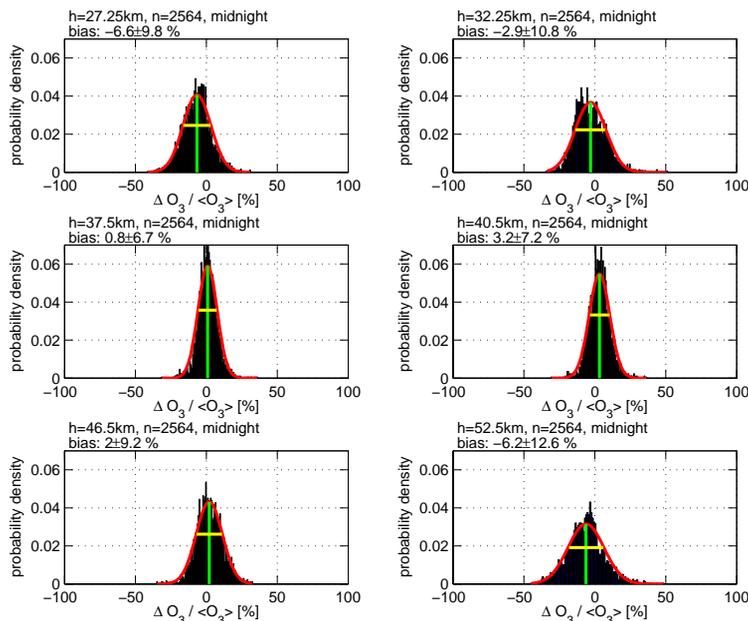
Fig. 4. Probability density function of the O_3 vmr differences Aura/MLS – SOMORA ($\Delta O_3/\bar{O}_3$) around midnight. The numbers of profile pairs n and the altitudes are given at the top of the graphs. The red line is the fit of the Gaussian normal distribution to the data. The green line indicates the bias (mean average), and the yellow line denotes the range of 2σ, where σ is the standard deviation.

Comparison and synergy of stratospheric ozone measurements

K. Hocke et al.
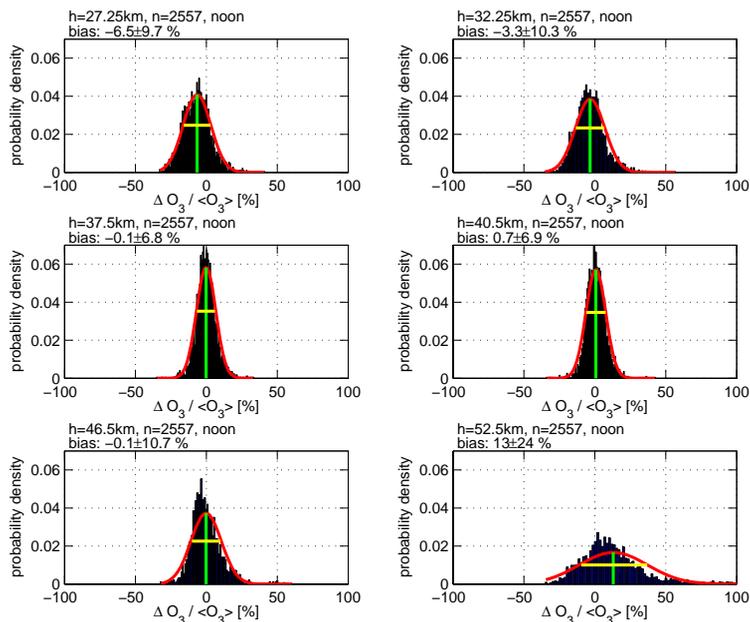
Fig. 5. Same as Fig. 4 but for the ozone differences around noon.
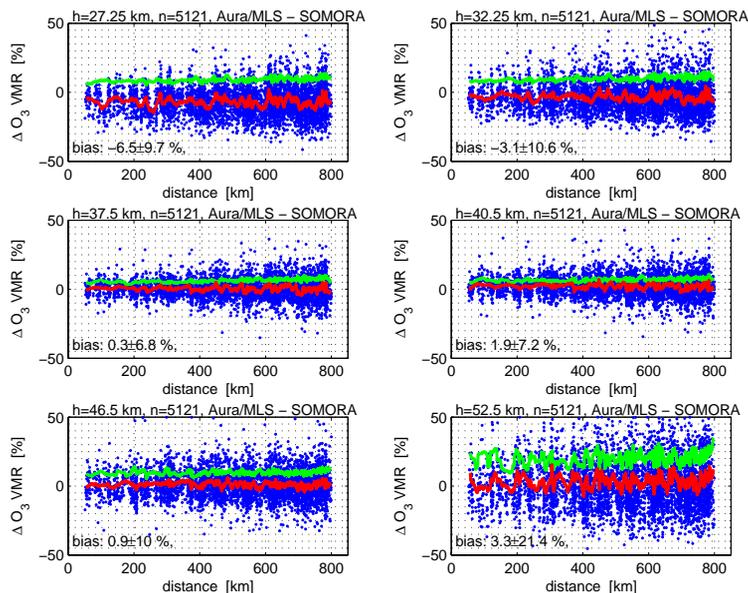
Fig. 6. O$_3$ differences (blue dots) as function of the horizontal distance between the sounding volumes of Aura/MLS and SOMORA. The red line indicates the mean bias (moving average over 50 profile pairs) as function of the horizontal distance while the green line denotes the related standard deviation σ.
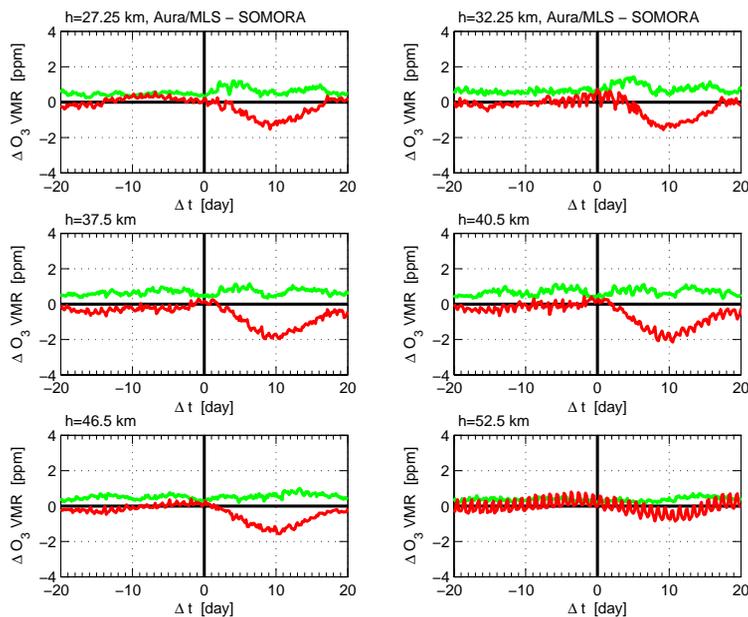
Fig. 7. Dependence of O_3 differences (Aura/MLS – SOMORA) on the time lag $\Delta t = t_{SOMORA} - t_{Aura/MLS}$. Nighttime Aura/MLS measurements from 10 January to 20 January 2005 have been selected. The red line denotes the mean bias, and the green line is the standard deviation.

Printer-friendly Version

Interactive Discussion
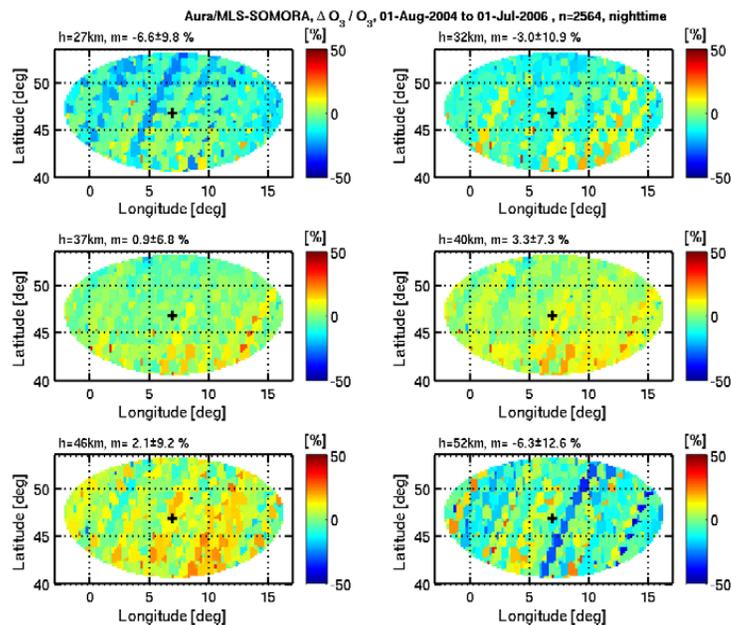
Fig. 8. Geographic map of nighttime ozone differences $\Delta O_3/\bar{O}_3$. The location of the ground station is indicated by the cross (center of the map). Faint stripes along the satellite sub-orbital tracks are observed.

EGU
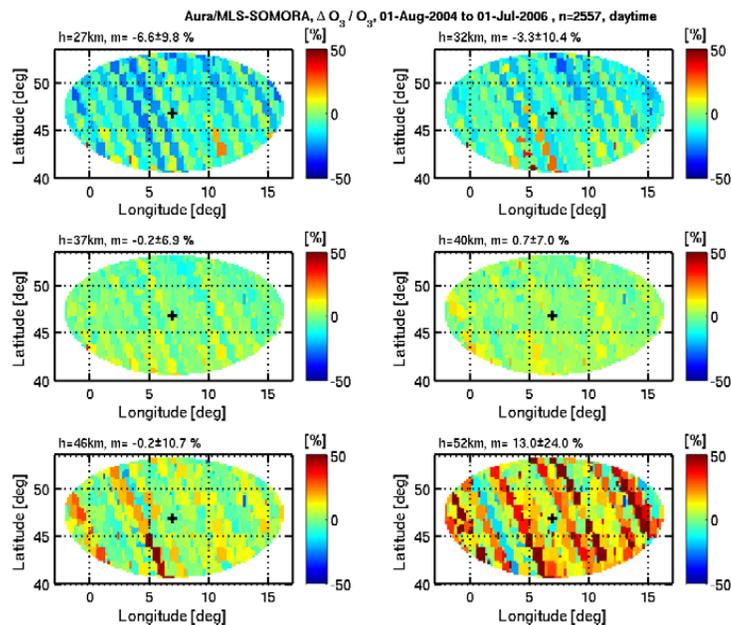
Fig. 9. Same as Fig. 8 but for daytime ozone differences.
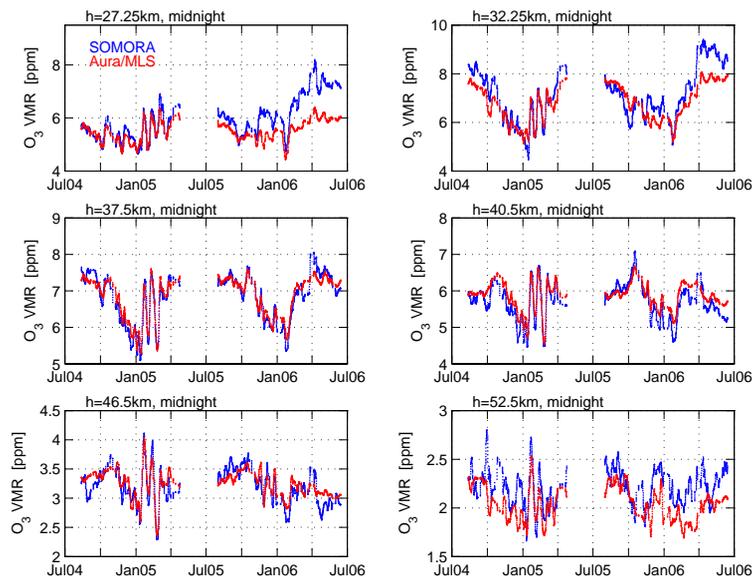
Fig. 10. Time series of nighttime O_3 VMR of SOMORA (blue line) and Aura/MLS (red line). Averaging kernel smoothing has been applied to the series of the Aura/MLS measurements which are coincident with the SOMORA measurements. Short temporal fluctuations (periods <4 days) are surpressed by a moving average over 30 data points of both time series.

EGU
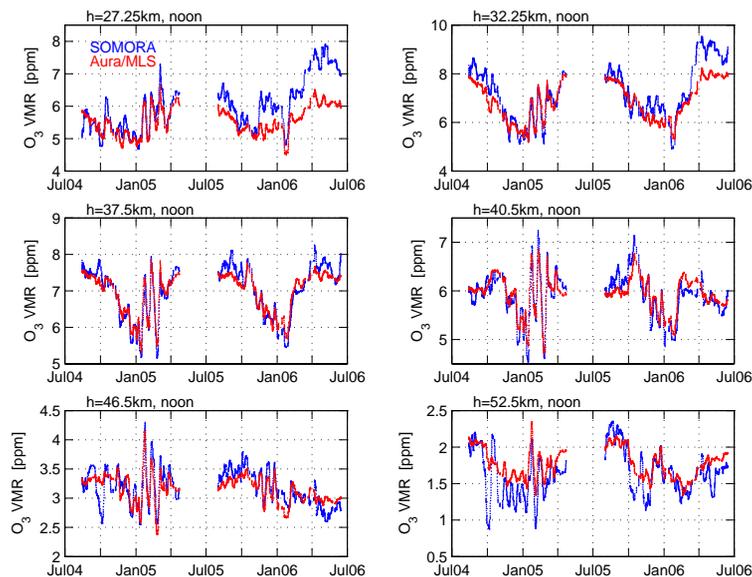
Fig. 11. Same as Fig. 10 but for the O_3 VMR measurements around noon. SOMORA is denoted by the blue line, and Aura/MLS by the red line.

Full Screen / Esc

Printer-friendly Version

Interactive Discussion
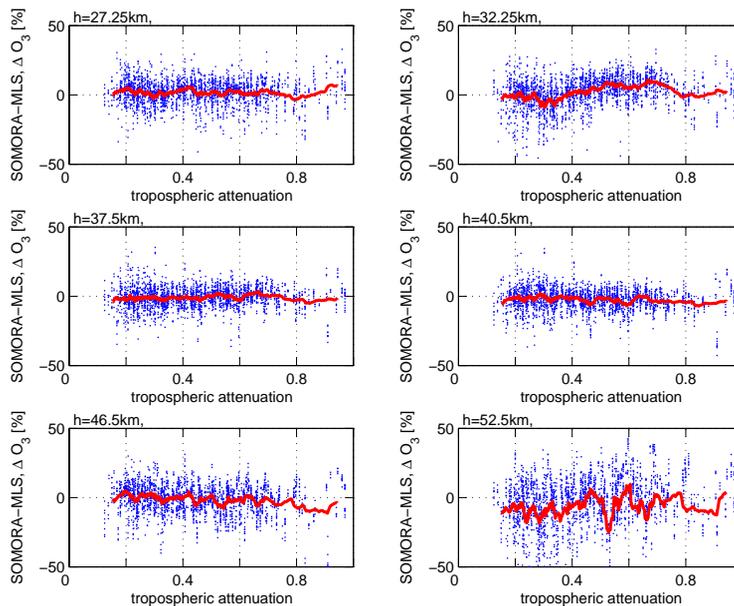
Fig. 12. Dependence of the relative O_3 differences on the tropospheric attenuation. The red line is the moving average over 100 differences.

EGU
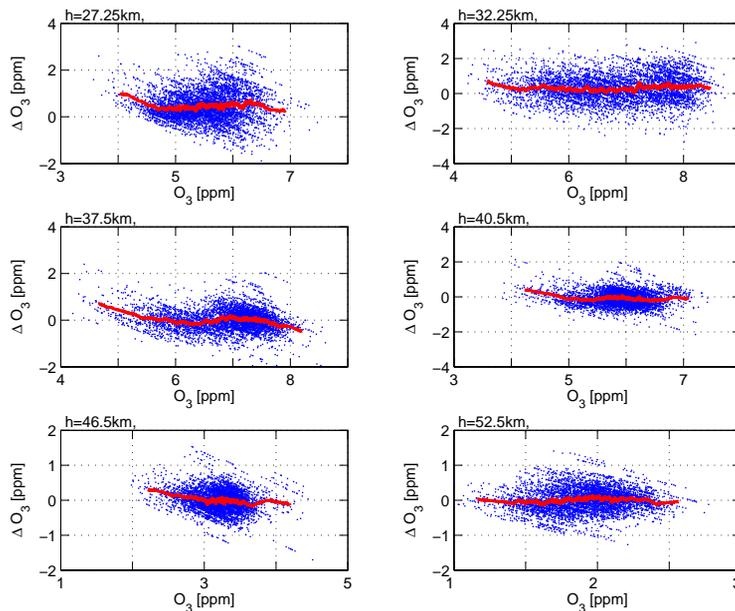
Fig. 13. O_3 differences (SOMORA – Aura/MLS) as function of O_3 (Aura/MLS) for all observations around noon and midnight. The red line is the moving average over 100 data points.
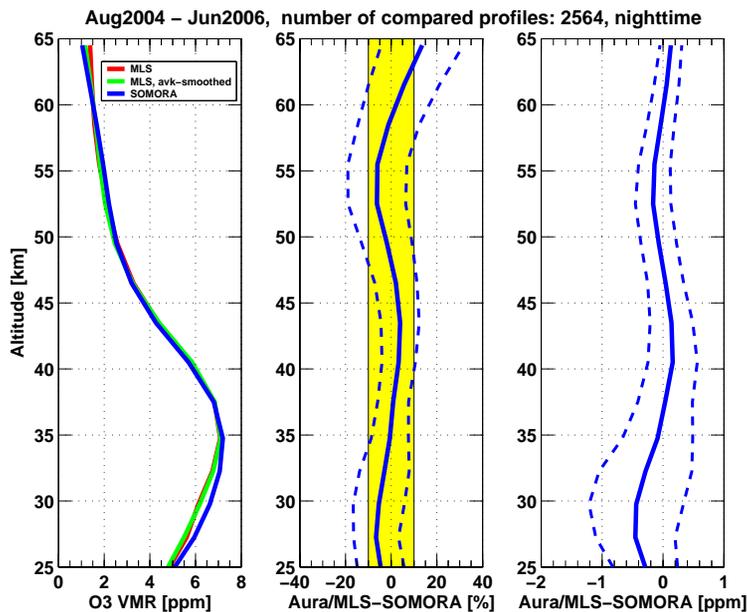
Fig. 14. Mean O_3 profiles of Aura/MLS and SOMORA around midnight averaged for the time from August 2004 to June 2006. The red line (left-hand-side) is the average of the original Aura/MLS profiles while the green line denotes the average of the MLS profiles when averaging kernel smoothing has been applied to each profile. Relative and absolute difference profiles (Aura/MLS – SOMORA) are shown in the middle and right-hand-side graph respectively. Averaging kernel smoothing has been applied to each Aura/MLS profile before subtraction of the coincident SOMORA profile.

EGU

Aug2004 – Jun2006, number of compared profiles: 2557, daytime
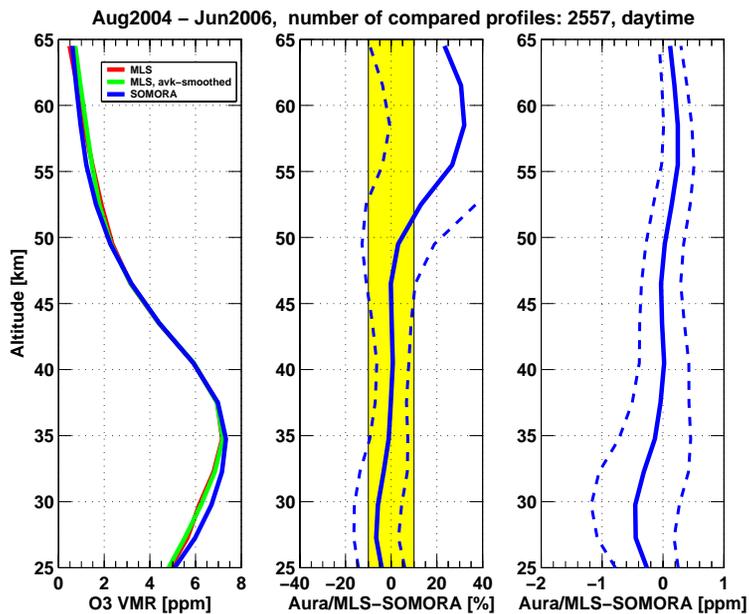
Fig. 15. Same as Fig. 14 but for the ozone measurements around noon.
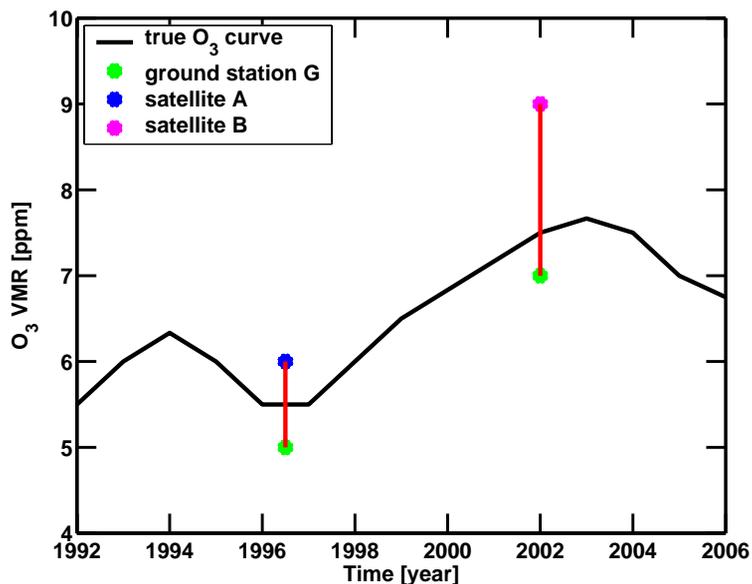
Fig. 16. Scheme of cross-validation by double differencing: Measurements of satellites *A* and *B*, separated in time, are compared by using the long-term data set of ground station *G* (the satellite measurements are nearby the ground station). The difference of lengths of the red lines is estimated to be the difference of the systematic errors of the satellites *A* and *B*. The black curve is the unknown time series of true ozone at a fixed altitude over the ground station.

EGU
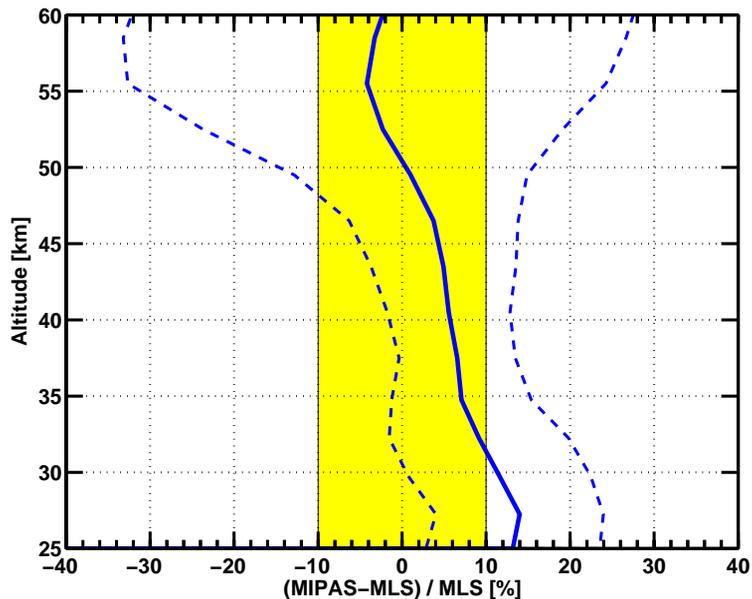
Fig. 17. Mean difference of the ozone difference profiles ENVISAT/MIPAS-SOMORA (n=116) and Aura/MLS-SOMORA (n=5121). The standard deviation of all differences is given by the dashed line. The yellow band indicates the ±10% area.

Title Page

Abstract | Introduction

Conclusions | References

Tables | Figures

◄◄ | ►►

◄ | ►

Back | Close

Full Screen / Esc

Printer-friendly Version

Interactive Discussion

EGU

**Comparison and
synergy of
stratospheric ozone
measurements**

K. Hocke et al.
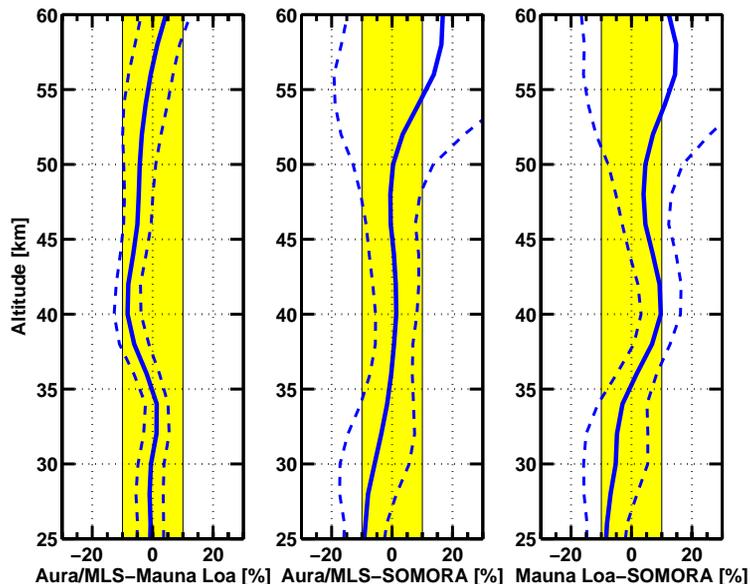
Fig. 18. Double differencing of the ozone measurements of the ground stations Payerne (46.82 N, 6.95 E) and Mauna Loa (19.5 N, −155.58 E) by means of the coincident measurements of the satellite experiment Aura/MLS from October to December 2005. The right-hand side panel depicts the ozone difference profile of the two ground stations which is the difference of the mean difference profile Aura/MLS-SOMORA (middle panel, n=803) and Aura/MLS-Mauna Loa (left-hand-side panel, n=160). The standard deviation of the differences is given by the dashed line. The yellow band indicates the ±10% area.
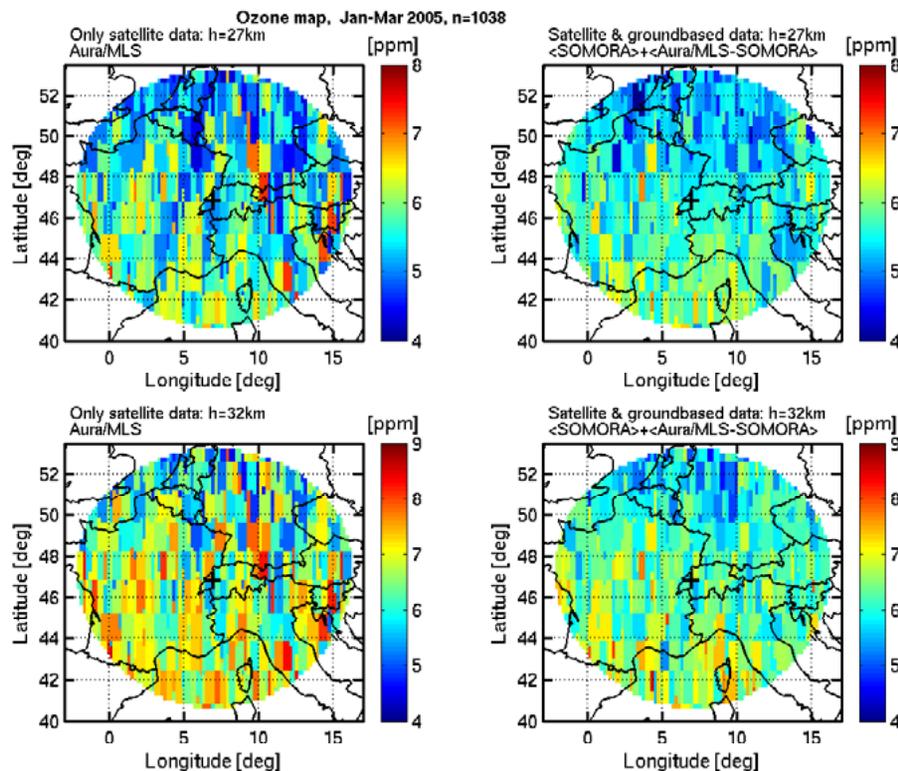
Fig. 19. Mean ozone maps around Payerne (black cross). The maps on the left-hand-side are calculated by using Aura/MLS profiles during January–March 2005. The temporal noise in the ozone maps is significantly reduced when the space-based measurements are combined with the ground-based measurements of the SOMORA radiometer in Payerne (ozone maps on the right-hand-side).

Title Page

Abstract | Introduction

Conclusions | References

Tables | Figures

◀ | ▶|

◀ | ▶

Back | Close

Full Screen / Esc

Printer-friendly Version

Interactive Discussion